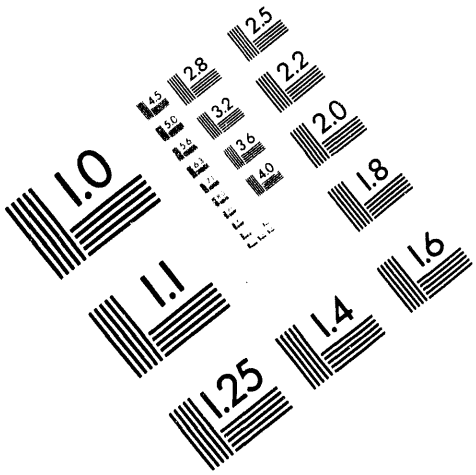

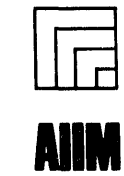

Association for Information and Image Management

1100 Wayne Avenue, Suite 1100
Silver Spring, Maryland 20910

301/587-8202

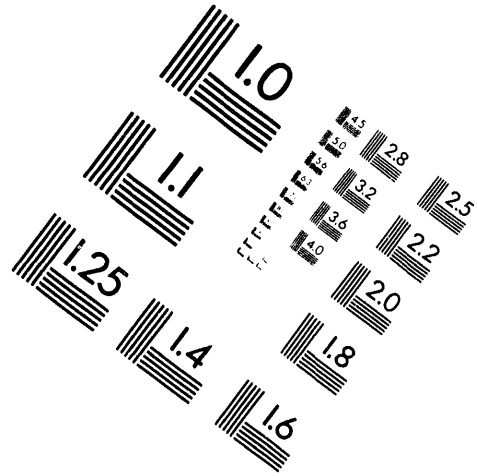

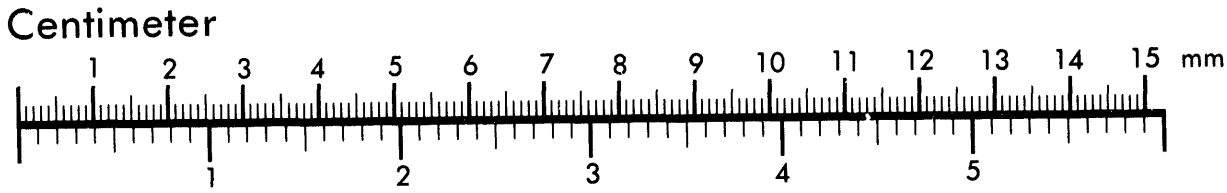

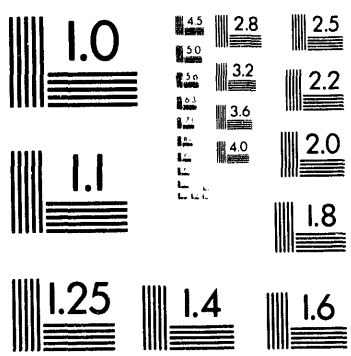

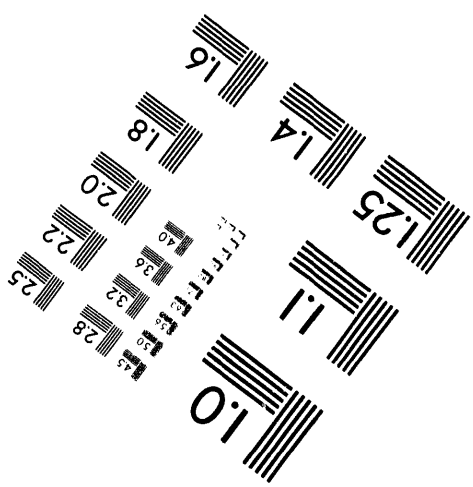

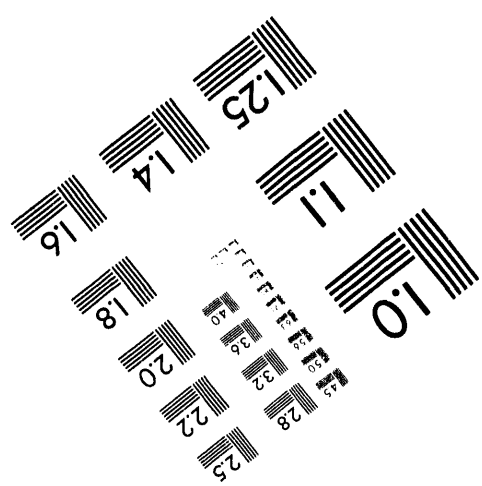

1 of 1

SAND94-0312
Unlimited Release
Printed August 1994

Distribution
Category UC-706

Measured Responses of Internal Enclosures and Cables Due to Burnthrough Penetration of Weapon Cases by Lightning

George H. Schnetzer and Richard J. Fisher
Electromagnetic Analysis and Testing Department
Sandia National Laboratories
Albuquerque, New Mexico 87185-0865

Michael A. Dinallo
Quatro Corp.
Albuquerque, New Mexico

Abstract

The electrical effects of lightning penetration of the outer case of a weapon on internal structures, such as a firing set housing, and on samples of a flat, flexline detonator cable have been investigated experimentally. Maximum open-circuit voltages measured on either simulated structures (126 V) or the cable (46 V) located directly behind the point of penetration were well below any level that is foreseen to create a threat to nuclear safety. On the other hand, it was found that once full burnthrough of the barrier occurred, significant fractions of the incident continuing currents coupled to both the simulated internal structure (up to 300 A) or to the cable sample (69 A) when each was electrically connected internally to case ground. No occurrence was observed of the injection of large amplitude currents from return strokes occurring after barrier penetration. Under circumstances in which small volumes of trapped gases exist behind penetration sites, rapid heating of the gas by return strokes occurring after burnthrough has been shown to produced large mechanical impulses to the adjacent surfaces.

Contents

Illustrations

Tables

Measured Responses of Internal Enclosures and Cables Due to Burnthrough Penetration of Weapon Cases by Lightning

1.0 Introduction

The electrical consequences of the penetration of a nuclear weapon case by lightning are being systematically investigated by Department 2753 as part of the Stockpile Lightning Analysis and Test (SLAT) program [1]. The possibility of charge transfer to components inside a weapon, such as a firing set housing or flat detonator cable, following burnthrough by lightning of the exterior case is of particular interest. In principle, if an internal component is electrically isolated from the case and receives sufficient charge, the result could be deleterious arcing inside the weapon, perhaps at a critical location remote from the site of the penetration. If the component is electrically grounded to the case, or if an arc occurs between the component and case, potentially large currents might result within the interior of the weapon.

A set of experiments was conducted to measure the charge transferred to components situated behind penetrations produced in a metal sheet by simulated lightning currents from the Sandia Lightning Simulator (SLS). In the experiments, the collector component was either a separate inner cylinder or a piece of flat flex detonator cable. The experimental arrangement allowed separate measurements of the voltage and currents injected onto the collector under conditions that approximated either an electrically open-circuit or short-circuit state of the component with respect to the exterior case. The responses were measured as a function of the spacing between the inside of the penetrated wall of the simulated weapon case and the surface of the collector, and under variations of the incident simulated lightning current parameters.

In these experiments, the fundamental assumption was that full burnthrough of a weapon case could occur. That is, the focus here was on the resulting electrical effects caused by a burnthrough, and not on whether or not such a burnthrough would actually occur in any particular situation. The latter question is being addressed elsewhere within the SLAT program and will be reported on separately [2].

The results of these investigations indicate that, even under quite severe conditions, charging of interior structures that float electrically with respect to the case is a negligible effect that does not produce voltages of sufficient magnitude to pose a safety threat to a weapon. On the other hand, under conditions in which an internal component is grounded to the case, it has been shown to be possible to inject a large fraction of the incident continuing current onto an internal component after penetration of the outer case occurs.

A collateral mechanical effect of some significance was also encountered during the course of these experiments. The design of the test object was such that a small volume of air was trapped between the aluminum outer wall of the simulated weapon case and the collector electrode behind it. During testing with simulated two-stroke flashes, the incidence of the second stroke caused rapid heating and expansion of the air behind the barrier plate. The resulting sudden overpressure was sufficient to cause significant outward deformation of the entire barrier plate. The degree of deformation is indicative of the development of a substantial mechanical force that could, under certain conditions, conceivably represent a threat to internal components that might be susceptible to mechanical shock.

2.0 Objectives

The specific objectives of these tests were

1. Determination of practical upper bounds on open-circuit voltages and short-circuit currents that can result on an internal component located directly behind the point of a lightning penetration of a weapon case, and

2. Characterization of the sensitivity of the above quantities to geometric parameters of the structure and to key parameters of the applied simulated lightning test currents.

3.0 General Description of the Experiments

The basic experimental arrangement is diagrammed in Figure 3-1 and is shown as it was implemented in Figure 3-2. It consists of a cylindrical aluminum outer case, which was bonded to the front of an aluminum instrumentation chamber. The front of the test cylinder was designed to allow the installation and replacement of an outer barrier plate of 0.047-in thick aluminum. Inside the outer cylinder was mounted a collector electrode in a manner that permitted adjustment of its separation distance d from the inside surface of the barrier. The adjustment feature was a threaded stem that screwed into a dielectric plate attached to the front piece of the instrumentation chamber. A locking nut was used to maintain the designated setting. The open-circuit voltages and short-circuit currents developed on the collector components were recorded during separate tests.

The objective of these tests required that full lightning burnthrough of the barrier plate would definitely occur. The attachment of the arc was, therefore, done in such a way as to ensure a burnthrough of the barrier plate in each case. For most of the testing, the gap between the pointed 0.156-in diameter output electrode of the simulator and the barrier was adjusted to be 0.25 in. This short an electrode gap is understood to result in somewhat of an overtest with respect to real lightning [2]. However, since the point of the present experiments was the investigation of the effects that occur behind a breach of the barrier, and not whether or not such a breach occurs in the first place, the fidelity of the burnthrough process itself was not of primary importance. Only in those cases in which it was found to be possible to inject current through an existing hole of dimensions comparable to or larger than the electrode separation distance was there some question that the validity of the results might be compromised by the use of too short an arc length. That situation was, therefore, revisited using a 1-in gap between the machine electrode and the barrier, an arrangement that has been elsewhere demonstrated to reproduce with good fidelity damage spots obtained on aluminum samples exposed to real lightning [2]. The results obtained under this second configuration were virtually the same as the earlier ones.

In addition to the above experiments, similar ones were carried out in which the interior components of interest were sections of flat, flexline detonator cables. In these tests, it was arranged that the cable samples lay directly behind the penetration site at a separation distance of 0.2 in from the back of the barrier plate, and the resulting common-mode voltages and currents that were developed on the samples were measured.

3.1 Open-Circuit Voltage Response Instrumentation

Measurement of open-circuit voltages interior to the test object was accomplished as shown in Figure 3-3. The voltage induced on the collector, V_C, given in terms of the recorded voltage, V_O, is

$$V_C = 2V_O[(C_S+C_1)/(C_S)], \tag{3-1}$$

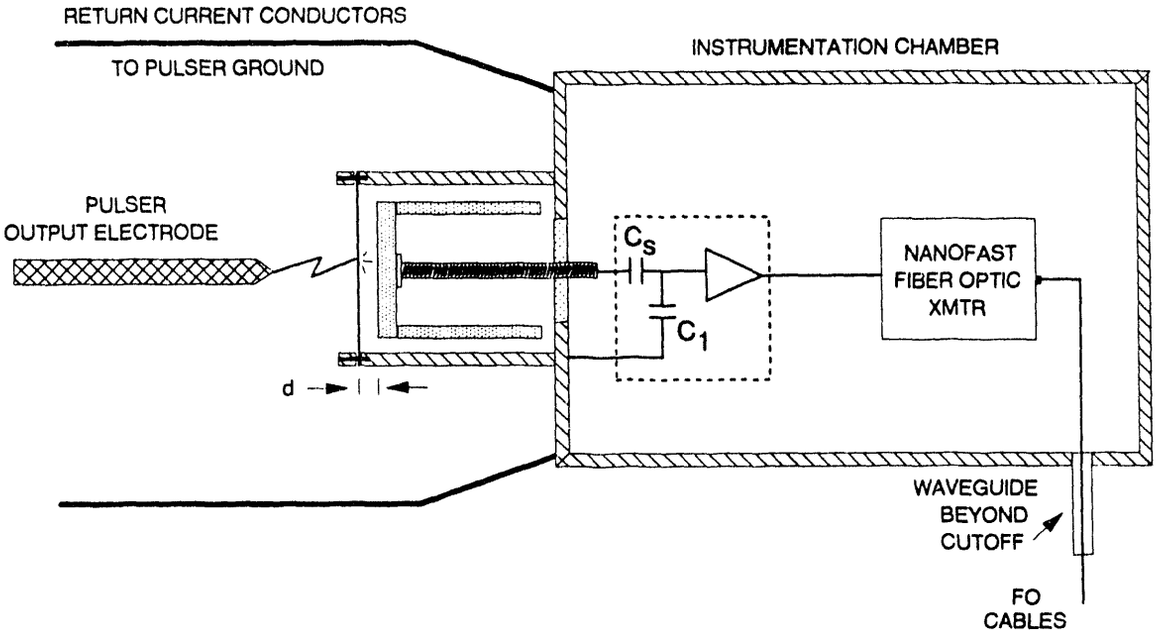

Figure 3-1 Basic configuration used during the burnthrough effects evaluation experiments

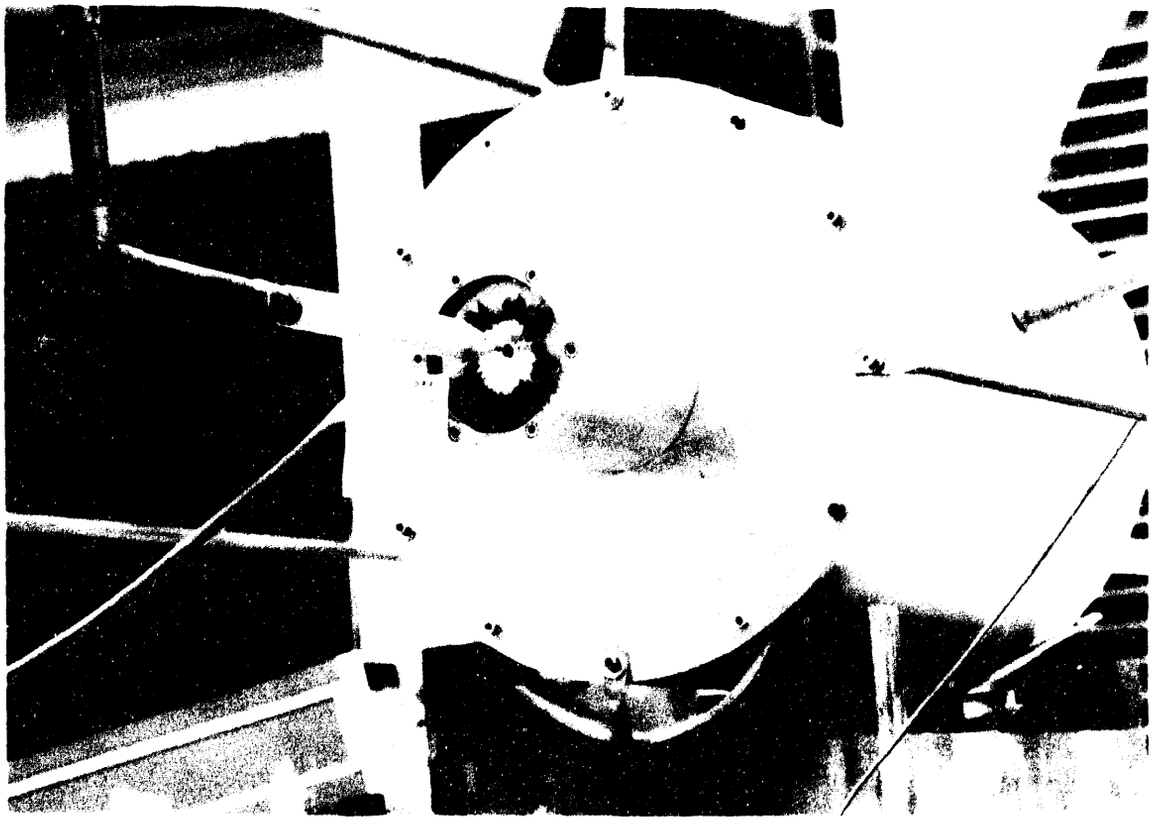

Figure 3-2 Photograph of burnthrough effects experiment configuration

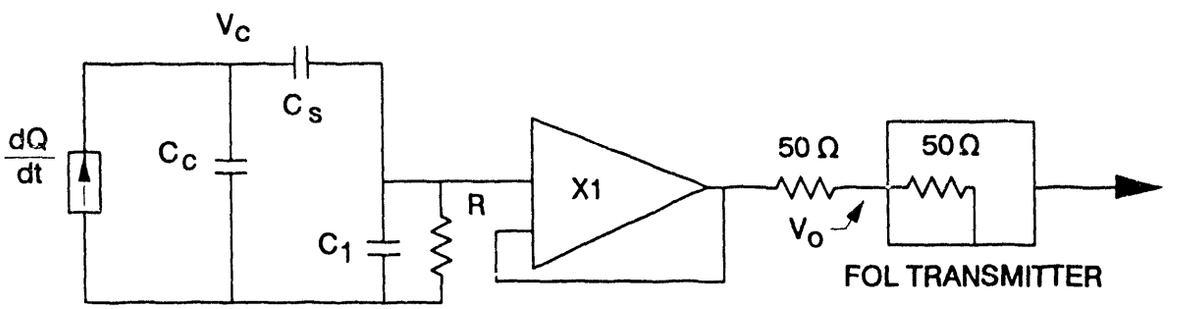

Figure 3-3 Technique used for measuring open-circuit voltages between the collector plate and the outer cylinder

and the net charge transferred to the collector is

$$Q = 2V_o\left[\frac{(C_s + C_1)}{C_s}\right]\left[Cc + \frac{C_s C_1}{C_s + C_1}\right]$$

$$Q \approx 2V_o\left[(C_c + C_s)(C_s + C_1)/C_s\right].$$

V_c and Q reflect the effect of the buildup of any retarding field in the gap between the barrier and collector during the flow of the test current. The values of C_c and C_s were determined by the design dimensions of the test object, as shown in Figure 3-4. Capacitance C_c was principally controlled by the length of the collector cylinder and was chosen to be representative of the typical capacitance of a major internal weapon component with respect to its surrounding case. C_s was set by the length labeled L in Figure 3-4. Teflon was used as the insulator/dielectric material both because its relative permittivity, 2.1, is approximately constant over all frequencies of interest and because of its high dielectric strength.

The acquirable charge and open-circuit voltages and charges were measured for $0.2 \leq d \leq 1.2$ in, where d is the separation distance between the barrier and the collector (Figure 3-4).

The high input impedance amplifier circuit designed for use in making the open-circuit voltage measurements is shown in Figure 3-5. The values of the capacitances and amplifier input resistance were

C_c = 64.7 pF (measured)

C_s = 19.8 pF (measured)

C_1 = 9.9 nF (measured)

R = 2 MΩ

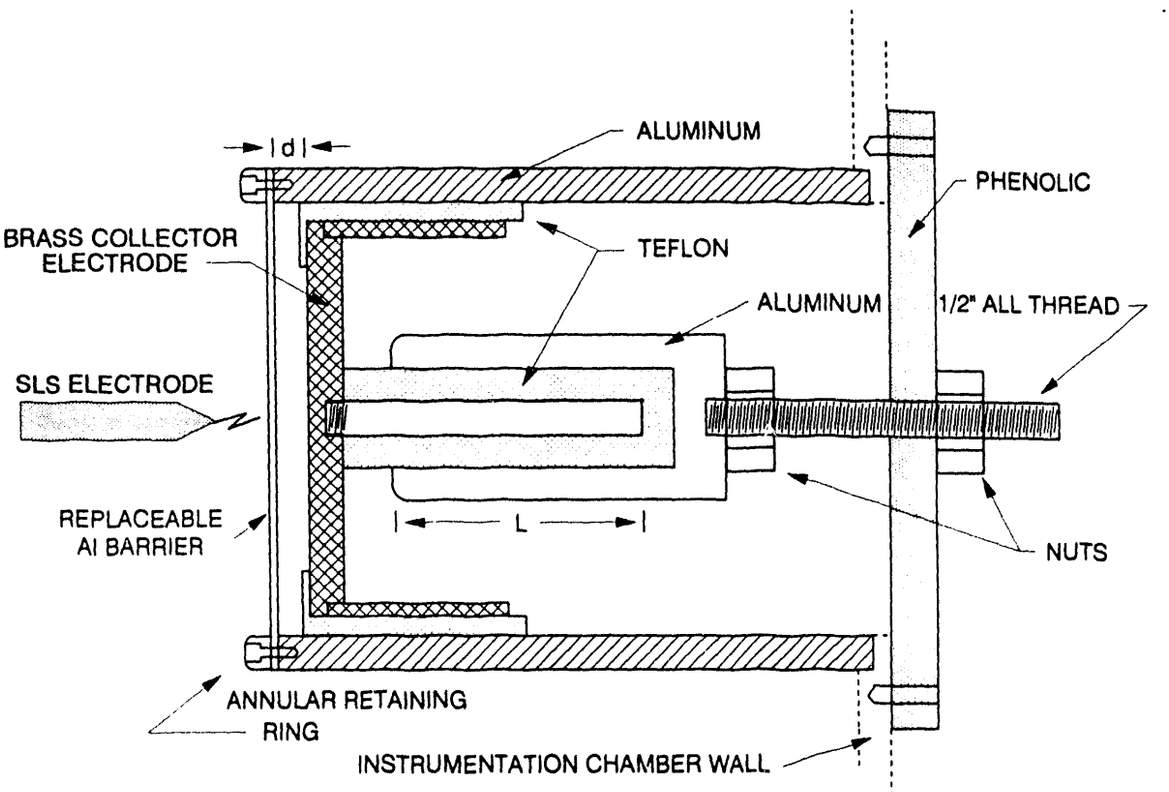

Figure 3-4 Details of the burnthrough effects experiment fixture

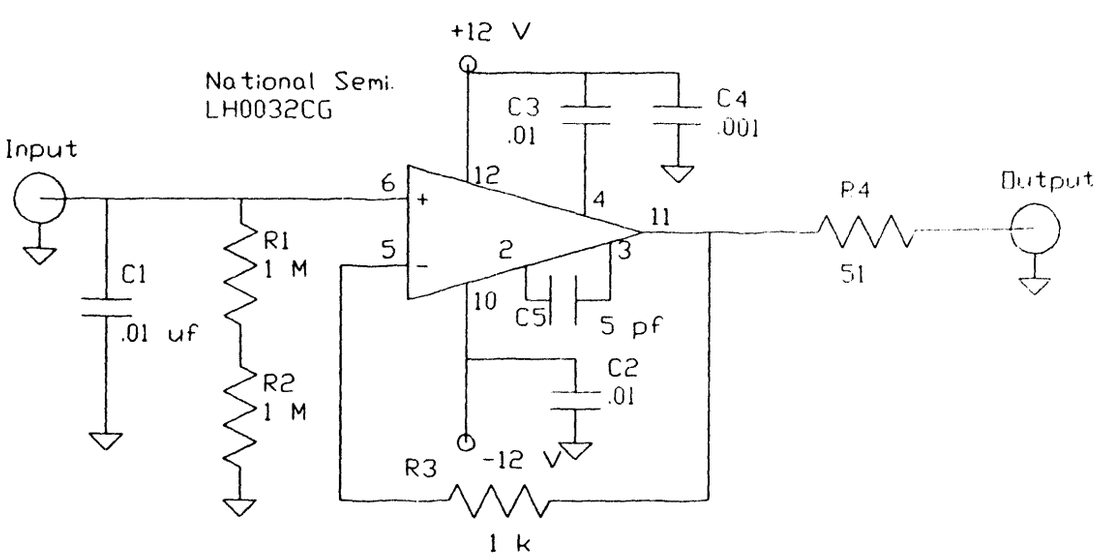

Figure 3-5 High impedance buffer amplifier used during the open-circuit voltage measurements shown in Figure 3-3

From (3-1) these values result in a measurement gage factor of 10^3 volts per volt output. The linear working range of the NanoFast FOLs is $| V_{in} | \leq 0.1$ volt. The value of C_1 was therefore chosen to maintain the response voltage at the output of the amplifier to within this range. The overall measurement upper frequency limit was approximately 25 MHz, which was set by the selected sampling interval of 20 ns on the Tektronix 7612D recording digitizer. The decay time constant was set by the input RC time constant of the amplifier, which was about 20 ms.

3.2 Short-circuit Current Response Instrumentation

The instrumentation employed in measuring the current flowing on the interior collector electrode is shown in Figure 3-6. The collector was tied to the case through a 5-mΩ current viewing resistor (CVR), the output of which was transmitted to the recording digitizer over a frequency modulated (FM) fiber optic data link with a low frequency bandwidth that extended to d.c. The early time higher frequency response was detected using a current viewing transformer (CVT) installed around the adjustment stem of the collector assembly as shown in the figure. The high frequency limit of that channel was 0.5 MHz, as set by the 1-μs sampling interval selected for its associated Tektronix 7612D digitizer.

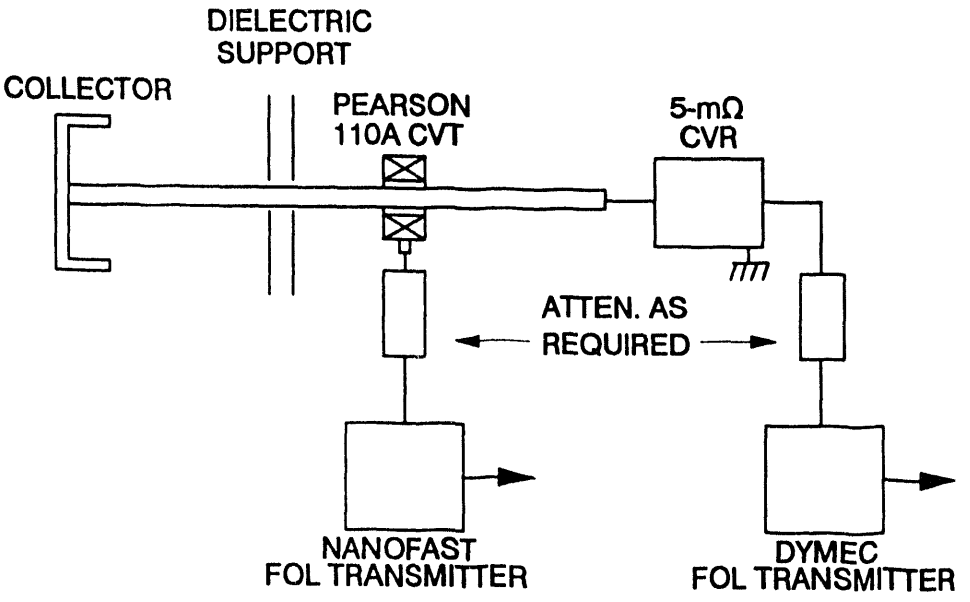

Figure 3-6 Instrumentation used for measuring short-circuit currents between the collector plate and the outer cylinder

4.0 Test Environment

An illustration is given in Figure 4-1 of a composite simulated lightning flash current of the type that is available from the SLS. The current consists of two simulated return strokes with continuing current during the interstroke interval and following the final stroke. This test current is referred to as a "full-flash" simulation. The second return-stroke and continuing current can be either separately included or left out as so chosen for any particular test. Peak amplitudes, rise times, full-width-to-half-maximum (FWHM) durations, and interstroke intervals can all be independently adjusted over fairly wide ranges that correspond to the distributions of their respective counterparts in real lightning.

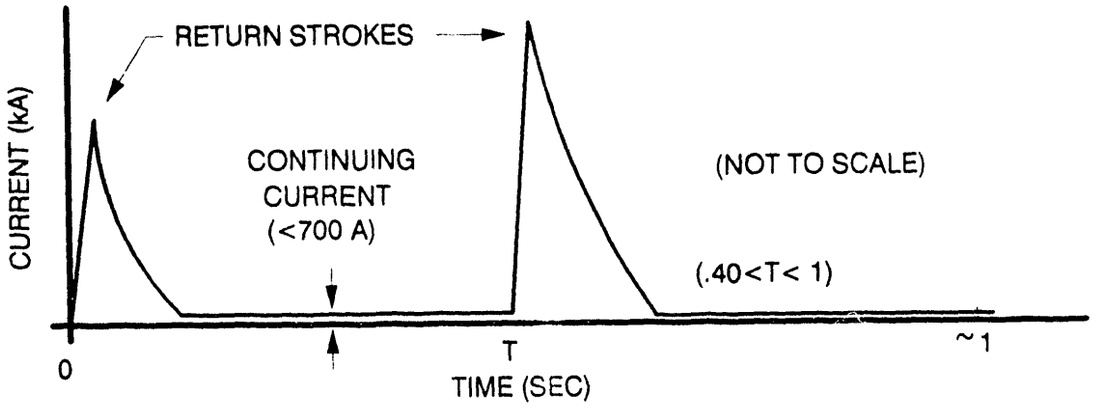

Figure 4-1 Simulated full-flash current waveform available from the SLS. Return-stroke amplitudes and rise times, interstroke intervals, and the initial amplitude of the continuing current are each adjustable.

4.1 The Sandia Lightning Simulator

In the SLS, return-stroke currents are produced by one or more of four individual Marx generators, which are housed in two separate tanks filled with insulating oil. These high voltage impulse generators can be operated in various combinations, and each feeds a common oil-filled transmission line connected to the machine output bushing. The unipolar waveform corresponding to real lightning is produced through the use of a laser-triggered shorting, or "crowbarring," switch across the Marx capacitors. The function of the crowbar switch is to short out the Marx voltage at or near the first peak of what would otherwise be an underdamped oscillating machine output current. This results in a current pulse with a rise time associated with the resonant frequency of the Marx capacitance and the discharge circuit inductance, followed by a decaying tail that is governed by the L/R parameters of the output circuit of the machine and test load. The nominal ranges of output parameters that are available are peak amplitudes from 20 to 250 kA, FWHM from 25 to 100 μs, and interstroke intervals from about 40 ms to a second. For loads with inductances less than about 3 μh, 10-to-90 percent rise times from 0.5 to 2 μs can be obtained. Figure 4-2a shows a typical simulated return-stroke current obtained from the SLS, and Figure 4-2b shows a sequence of return-stroke currents measured directly at the base of the lightning channel of a real flash, along with an expanded presentation of the first of the strokes on a faster time scale for comparison with Figure 4-2a. The ringing that appears just after the peak of the simulated return stroke is due to residual energy within the Marx capacitance and inductance following crowbarring.

Continuing current is provided from a large motor-generator set, the output of which is coupled into the simulator output circuit through a large pulse isolation inductor. Prior to the test shot, the set is spun up in the motor mode to a designated spin rate. Just before the shot, the set is switched to the generator mode and

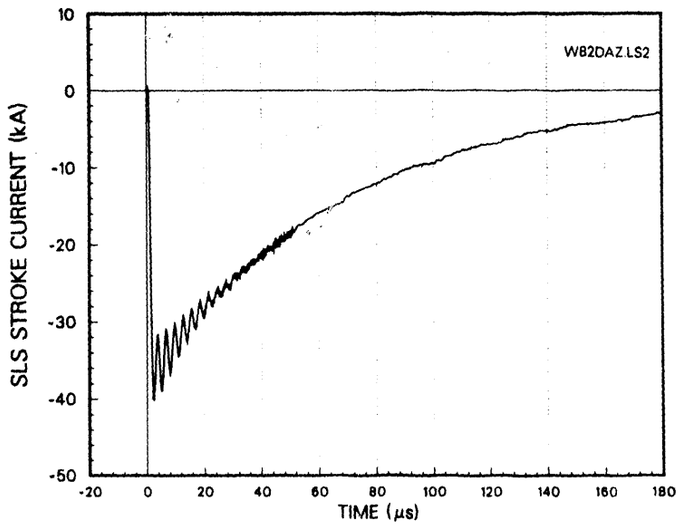

(a)

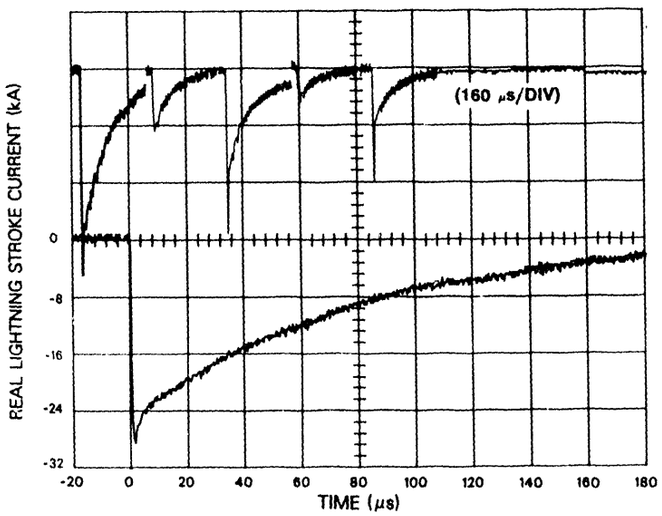

(b)

Figure 4-2 (a) Simulated lightning return-stroke current obtained from the SLS; (b) five return-stroke currents measured at the base of a real lightning channel (top), and expanded plot of the first stroke current (bottom)

is then allowed to spin down under its own inertia during the course of the test event, producing an approximately exponentially decaying output current. Initial continuing current values of up to 700 A can be obtained, corresponding to the ninety-ninth percentile severity in a natural lightning flash [3]. Figure 4-3 shows an example continuing current produced by the SLS.

The total current applied to a test object is recorded by summing the outputs of three low impedance coaxial current viewing resistors (CVR) that are inserted into the current return path to pulser ground. The recording arrangement for these signals is shown in Figure 4-4.

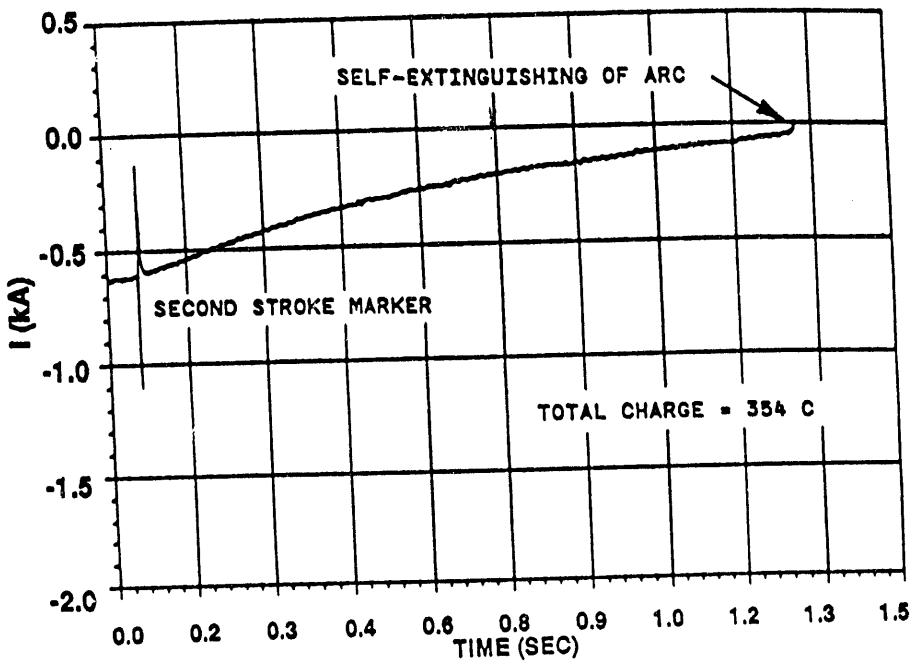

Figure 4-3 Exampie of severe continuing current obtained from the SLS

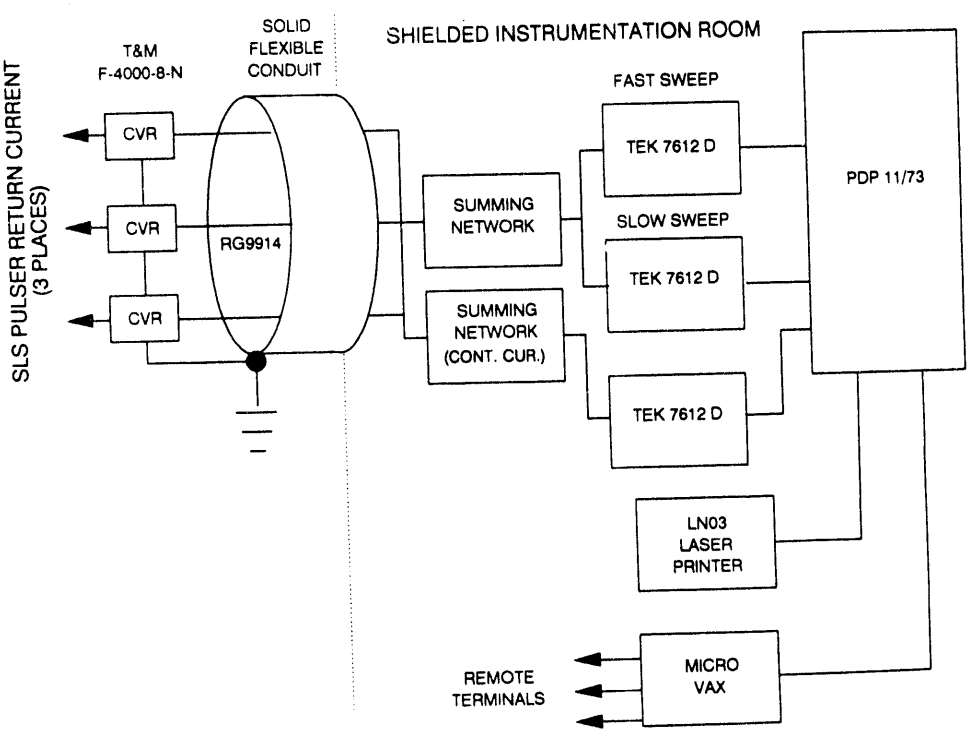

Figure 4-4 SLS output current recording instrumentation

5.0 Measured Internal Voltages

5.1 Return Strokes to the Site of a Pre-existing Small Hole

It is well documented that return-stroke currents not accompanied by following continuing currents do not cause penetration of metallic sheets by the mechanism of thermal burnthrough [e.g., 4-6]. (On the other hand, the forward shockwave of a severe return-stroke current is definitely capable of breaching thin metallic sheets [7].) Nevertheless, during the present experiments, an initial set of tests was carried out to investigate the electrical coupling that takes place when a return stroke impinges on the site of a small existing penetration. This possibility exists because the presence of the hole results in a marginally enhanced local electric field at that site, and this increased electric field provides inducement for the attachment to take place at that spot. The charge transferred to the collector through a pre-drilled hole of 0.125-in diameter in the 0.047-in thick aluminum barrier was measured as a function of barrier-collector distance d. The 0.25-in pointed tungsten output electrode of the SLS was positioned directly over the hole in the barrier with an electrode-to-surface spacing of 0.25 in. The results are summarized in Table 5-1.

Even when linearly extrapolated to correspond to a very severe return-stroke current in excess of 200-kA peak amplitude, the present results do not indicate any significant threat of coupling to the interior of a weapon.

Table 5-1.
Charge Transfer to a Collector Behind a 0.125-in Hole

Test Shot ID	I_p [1] (kA)	d (in)	Measured Charge (nC)	Equivalent Peak Voltage (V)[2]	Comments
1971	43.0	0.2	8.7	0.102	Considerable Al splatter on collector
1972	49.9	0.4	8.0	0.094	Considerable Al splatter on collector
1973	50.4	0.8	0.3	0.004	Very little Al splatter

[1] Peak amplitude of the applied current

[2] Peak voltage between the internal collector and the surrounding case corresponding to the listed charge

5.2 Single Return Strokes Followed by Severe Continuing Current

Summarized in Table 5-2 are the peak values of charge transferred to the collector electrode and corresponding collector voltages with respect to the exterior case that were measured in response to applied single return strokes followed by severe continuing currents. Return strokes of 50-kA and 100-kA peak amplitudes (with FWHM values of about 50 and 200 μs, respectively) were employed. In each case, the continuing current had a nominal initial value of 500 A, an exponential decay as shown in Figure 4-3, and a duration to the self-extinguishing of the arc of more than 1 second. Also, in all cases, a 0.156-in diameter pointed tungsten electrode was used, with gap length between its point and the aluminum barrier surface of 0.25 in.

Table 5-2.
Collector Responses due to Single Return Strokes Followed by Severe Continuing Currents

Test Shot ID	I_p[1] (kA)	Initial I_{cc}[2] (A)	d (in)	Measured Charge (nC)	Equivalent Peak Voltage (V)[3]
1978	49	445	0.2	<0.35	<4.1
1981	46	426	0.2	1.8	21.4
1982	51	421	0.2	4.0	47.2
1993	49	452	0.4	1.3	18.2
1995	50	453	0.4	1.9	26.6
2003	50	468	0.8	1.0	15.0
2004	50	456	0.8	1.8	27.0
2001	51	468	1.2	1.1	16.0
2002	41	461	1.2	1.8	31.3
1985	98	510	0.2	4.8	56.6
1986	92	430	0.2	6.5	76.7
1987	83	510	0.4	2.0	28.0
1988	92	510	0.4	1.5	21.0
1989	93	500	0.4	0.7	10.5
1990	90	510	0.4	0.5	7.5

[1] Peak amplitude of the applied return-stroke current

[2] Initial amplitude of the exponentially decaying continuing current

[3] Peak voltage of interior collector electrode with respect to the outer cylinder

Typical waveforms of the responses are given in Figure 5-1, in which a progression of recorded collector voltages are presented for various barrier-to-collector spacings, d. It is noted that penetration of the aluminum barrier, as marked by the onset of the collector voltage signal, occurs significantly later with respect to the initiation of the test current for d = 0.2 in than it does for d = 0.4 or 0.8 in. Why this is the case has not been quantitatively investigated, since time to penetration was not an issue of interest in the present investigation. Qualitatively, it is thought to be related to the tighter thermal coupling between the barrier and the collector mass that accompanies a separation of only 0.2 in. With the increased thermal relief provided by the collector under this condition, a longer time to full melt-through of the barrier might be expected.

Of primary interest are the levels of the peak voltages, the maximum of which was of the order of 80 V. This value occurred during shot S1986, which was conducted with d = 0.2 in. The explanation for the observed voltages and their characteristic waveforms appears to be as follows. Initially following the breach of the barrier, charge is freely transported across the intervening space to the collector electrode. The collector then begins to increase in potential with respect to the outer case. However, this process is quickly interrupted as the arc plasma, which is highly electrically conducting due to its ionized state, fills the intervening space and, in effect, produces an electrical short between the collector and the barrier. In accordance with this explanation, the periods of oscillating signal appearing at later times in the records corresponding to 0.4- and 0.8-in spacings probably reflect plasma variations within the volume between the barrier and the collector. As these changes occur, the collector is alternately permitted to receive charge and

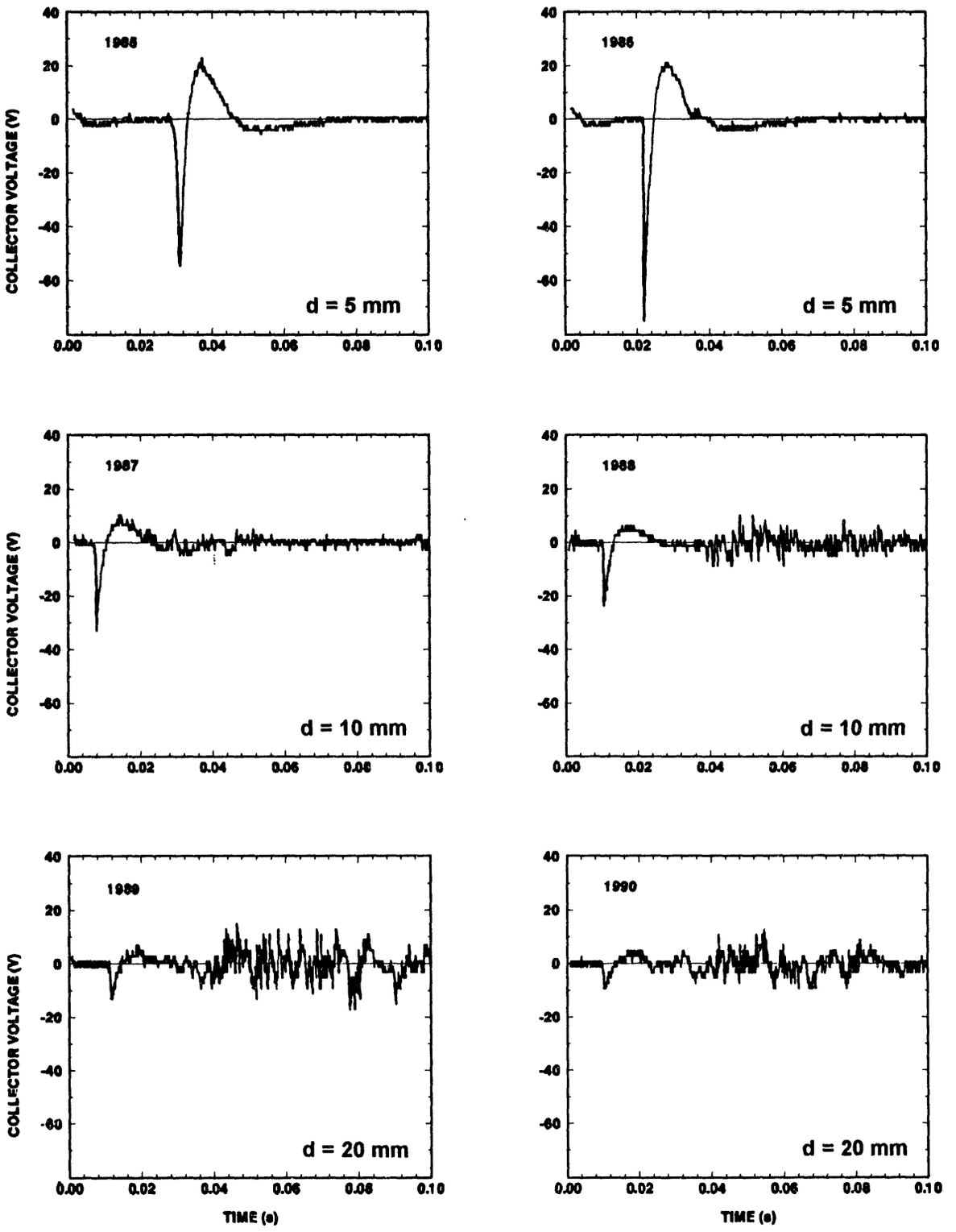

Figure 5-1 Example collector voltage waveforms measured for different distances between the collector electrode and the inside surface of the barrier plate

is then discharged once again as the plasma re-establishes contact with both surfaces. The fact that these late time variations are more prominent in the records corresponding to the larger interelectrode spacings appears to be consistent with the proposed interpretation.

In the records shown in Figure 5-1, the details of the collapse of the voltage are undoubtedly distorted due to the 20-ms time constant of the measurement circuit. However, the fast changing portions, including the rise to peak, are well characterized.

5.3 Effects of Subsequent Strokes and Barrier to Collector Separation

The typical time history of the major current components of a two-stroke lightning flash is illustrated in Figure 5-2. In such a flash, continuing current often accompanies one or more of the component return strokes. Following cessation of the continuing current, a quiescent period of duration of tens of milliseconds occurs before the initiation of the next stroke. This pattern may be repeated many times throughout the course of the flash, as is illustrated in Figure 5-2, which is a plot of the current measured directly at the base of the channel of a real lightning flash. The sensitivity of the recording channel in this particular instance was adjusted to capture the details of the low amplitude continuing current components, so the return-stroke components appear as fast spikes that exceed the saturation point of the instrumentation at about 1 kA. Of specific interest in the next set of tests was what happens electrically behind a penetration site when a subsequent stroke occurs.

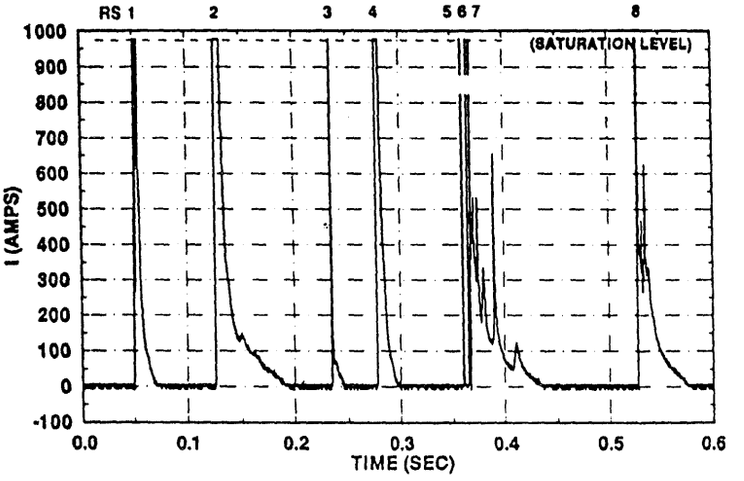

Figure 5-2 Example lightning current measured at the base of a rocket- triggered lightning flash; sensitivity was set to capture details of the continuing currents, resulting in instrumentation saturation by the much higher amplitude return strokes

This scenario was simulated by applying simulated two-stroke flash currents comprised of a sequence of 50- and 100-kA amplitude strokes with 500-A intervening continuing current. The interstroke interval was 100 ms, which ensured that full penetration of the barrier plate would take place prior to initiation of the second stroke. Two test shots of this kind were conducted with the barrier-to-collector spacing adjusted to each of three distances: 0.2, 0.4 and 1.2 in. The resulting measured voltages obtained during this sequence are listed in Table 5-3, and the associated waveforms are given in Figure 5-3. In that figure, the responses to the second stroke occur at or about 100 ms into each of the records. The smaller responses occurring earlier at or about 10 to 20 ms are those corresponding to the initial penetration of the barrier following the first stroke. It is evident that for d = 0.4 in (and presumably less), the voltage transients

Table 5-3.
Collector Voltages Produced by Subsequent Return Strokes Following Barrier Penetration[1]

Test Shot ID	Second Stroke Response[2](V)	d (in)	Comments
1994	126	0.4	Significant outward bulging of the barrier plate
1996	109	0.4	Same
1991	23	0.8	No bulging of plate
1992	30	0.8	Same
1999	16	1.2	No bulging of plate
2000	64	1.2	Same

[1] In each case, the applied test current consisted of a two-stroke sequence of 50/100-kA strokes with continuing current of 500-A initial amplitude; interstroke interval was 100 ms

[2] Peak collector voltage with respect to the outer case

developed on the collector due to the second strokes are substantially larger than those resulting from penetrations following single strokes and their associated continuing currents. On an absolute basis, however, the maximum transient of 126 V (S1994) is still about a factor of ten below a level that would begin to raise significant concerns over weapon safety.

The behavior of the data shown in Figure 5-3 appears to be consistent with the proposed interpretation given in Section 5.2. That is, following initial penetration, plasma variations within the intervening space between the barrier and the collector result in periodic charging and discharging of the collector with respect to the case. At the smallest separation distance of 0.4 in, the shockwave accompanying the second return stroke evidently blew aside or otherwise altered the existing plasma and permitted a relatively large amount of charge to transit the gap before the intervening space was once again shorted out by the ionized arc plasma. At the larger separation distances of 0.8 and 1.2 in, it is speculated that the increased volume of gas in the space apparently acted as a buffer of some sort, so that the existing plasma was not fully swept out and was therefore capable of continuing to hold the collector and case at nearly the same potential, even during the stroke itself.

This view of the phenomena taking place within the barrier-to-collector volume is further supported by the observed mechanical responses of the barrier plate. In each case following a test with the spacing set at d = 0.4 in, the barrier plate was found to have bulged out significantly towards the SLS electrode (Figure 5-4), thereby indicating the development of a considerable sudden overpressure behind the barrier caused by heating of the trapped gases there. This effect only occurred during the double-stroke simulations, and it was only significant in the 0.4-in spacing configuration.

This mechanical response raises the possibility of an additional weapon safety threat mechanism. That is, should lightning attachment occur at a particular site on a weapon case behind which there exists a small volume of confined space, a severe mechanical shock could be imparted to adjacent components. Quantitative evaluation of the consequences of such a scenario would appear to be possible only on a case-by-case basis, but such an outcome is something that should be taken into account during lightning assessments of individual weapons.

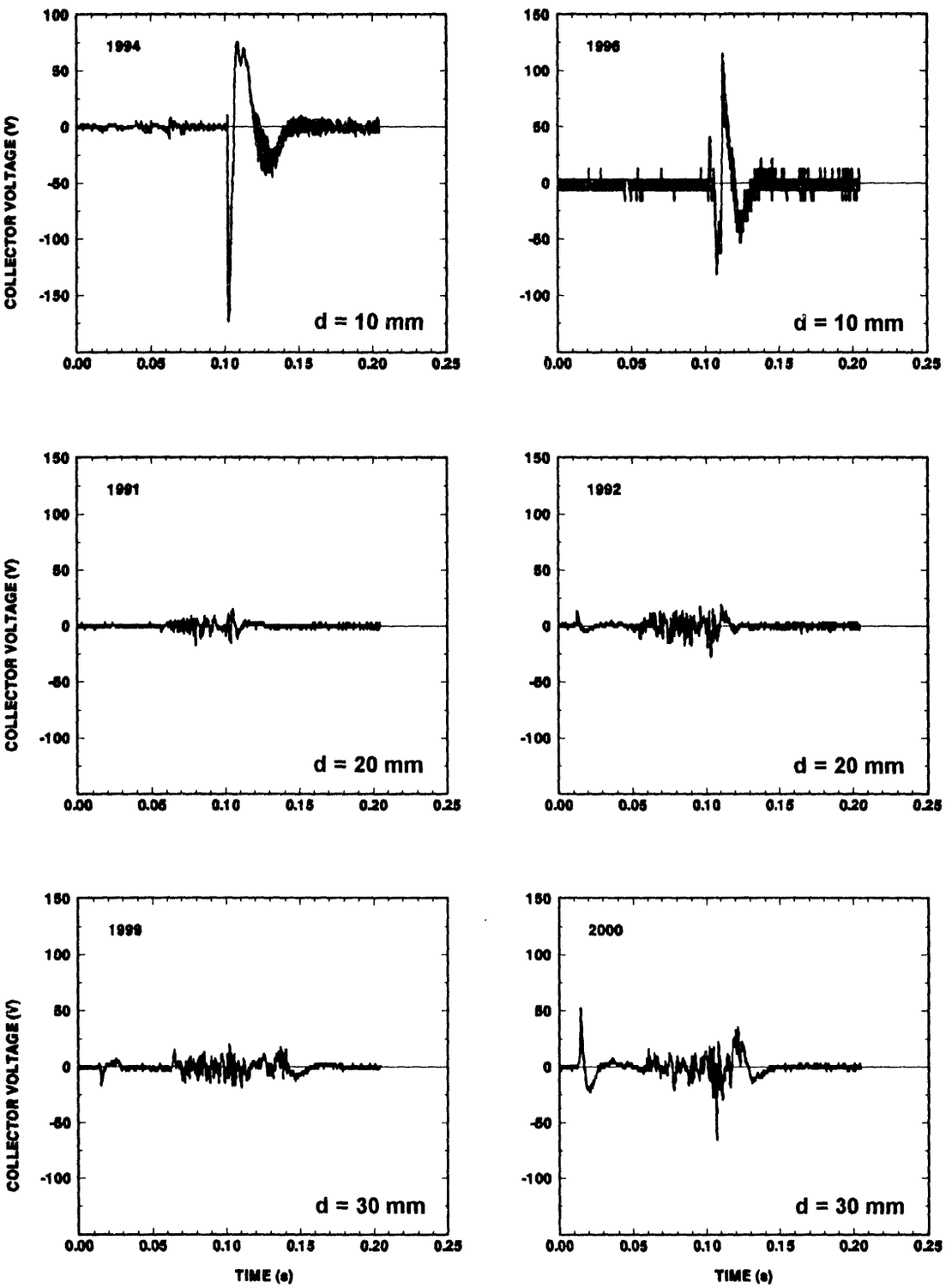

Figure 5-3 Collector voltage waveforms recorded during two-stroke flash simulations with intervening continuing current.

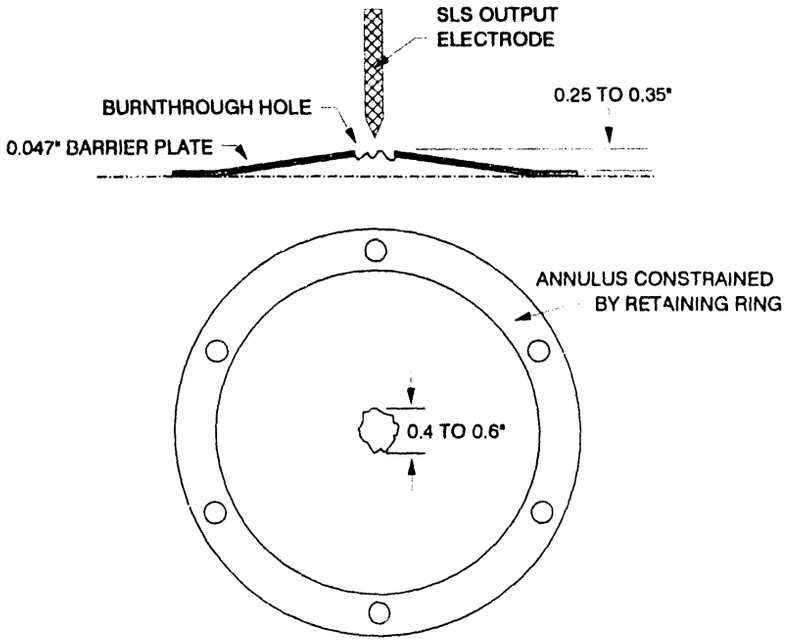

Figure 5-4 Outward deformation of barrier plate occurring on second stroke of two-stroke flash simulations with barrier-to-collector spacing of 0.4 in

6.0 Measured Internal Currents

Using the instrumentation discussed in Section 3.2 for measuring currents internal to the simulated weapon case, a sequence of test shots was conducted as listed in Table 6-1. The applied current in each case consisted of either one or two return strokes with severe continuing current. The initial amplitudes of the continuing currents were nominally 500 A.

Examples of the early-time short-circuit response current flowing between the collector electrode and the outer cylinder are given in Figure 6-1. In each case, t = 0 corresponds approximately to the start of the second return stroke. The same data are displayed in Figure 6-2 on a much longer time scale that covers the entire response. In the longer time scale plots, the time of the first return stroke was at approximately t = 100 ms. As is evident from the data, no significant current flow was detected prior to the onset of the second stroke.

The data plotted on the long time scale make it clear that, following penetration of the barrier, a significant fraction, if not all, of the continuing current attached to the collector through the hole created by current flowing between the first and second strokes. The data of Figure 6-2 also reveal that, in most cases, the continuing current flow was interrupted at an acoustic rate which is thought to be related to the characteristics of the cavity between the barrier plate and the collector electrode. This interaction produced a clearly audible sound during the test shots on which it occurred. During two test shots (3835 and 3855), a layer of 0.063-in thick silicone rubber was installed over the face of the collector plate, held tightly in place against the collector by the lip of the Teflon insulator between the collector and the outer case (see Figure 7-1). No detectable current beyond measurement noise was observed on either shot.

As was discussed in Section 5.3, during the two-stroke simulations, sudden heating of the gases trapped in this cavity by the second return stroke resulted in a bulging out of the barrier plate towards the pointed tip of the output electrode of the SLS. Since the typical diameter of the hole that was burned in the barrier plate during these tests was between 0.4 to 0.6 in, the result of this outward deformation of the plate

Table 6-1.
Measured Short Circuit Currents Between the Collector Electrode and the Outer Case

Test Shot ID	d[1] (in)	EB GAP[2] (in)	1st RS (kA)	2nd RS (kA)	I_{cc}[3] (A)	Meas. I_{sc}[4] (A)	Comments
3426	0.2	0.25	53	NA	472	139	
3427	0.2	0.25	56	NA	---	77	Cont. current data lost
3428	0.2	0.25	53	NA	482	52	
3832	0.2	0.25	50	NA	519	39	
2056	0.4	0.25	51	107	490	75	Interstroke int. = 100 ms
2057	0.4	0.25	54	109	480	105	
3833	0.4	1.0	46	NA	534	53	
3834	0.4	1.0	55	NA	556	122	
3844	0.2	1.0	55	94	550	238	
3848	0.2	1.0	55	89	500	169	
3853	0.2	1.0	50	88	500	307	
3854	0.2	1.0	49	83	500	55	
2058	0.8	0.25	50	92	500	95	
2059	0.8	0.25	52	111	500	25	
2060	0.8	0.25	50	109	500	83	
2061	0.8	0.25	54	108	500	102	
2064	1.2	0.25	55	116	500	65	
2062	1.2	0.25	46	120	500	<2	
3835	0.4	1.0	56	NA	541	0	Rubber layer installed
3855	0.2	0.25	53	88	500	0	Rubber layer installed

[1] Barrier-to-collector spacing

[2] SLS electrode-to-barrier gap

[3] Initial amplitude of continuing current

[4] Maximum recorded collector-to-case short circuit current

was that the tip of the SLS electrode ended up positioned inside the hole itself. This outcome raised the issue as to whether the continuing current flowing after the second return stroke had been artificially directed to attach to the inner collector as an artifact of the initially short gap (0.25 in) between the SLS electrode and the aluminum barrier plate. This portion of the testing was therefore repeated with a 1-in electrode spacing, which has been shown elsewhere in the SLAT program to replicate well damage spots obtained on metallic samples that had been exposed to artificially triggered natural lightning [2,6]. As indicated in Table 6-1, the results obtained using this longer electrode spacing show that, even under these conditions, coupling of current onto the internal collector electrode still occurred. It is therefore concluded that the injection of a significant fraction of the continuing current incident on the weapon into its interior following a burnthrough is a possibility that must be taken into account under certain weapon/lightning interaction scenarios. Further, additional return strokes may also have some fraction of current injected through the existing path to the weapon interior.

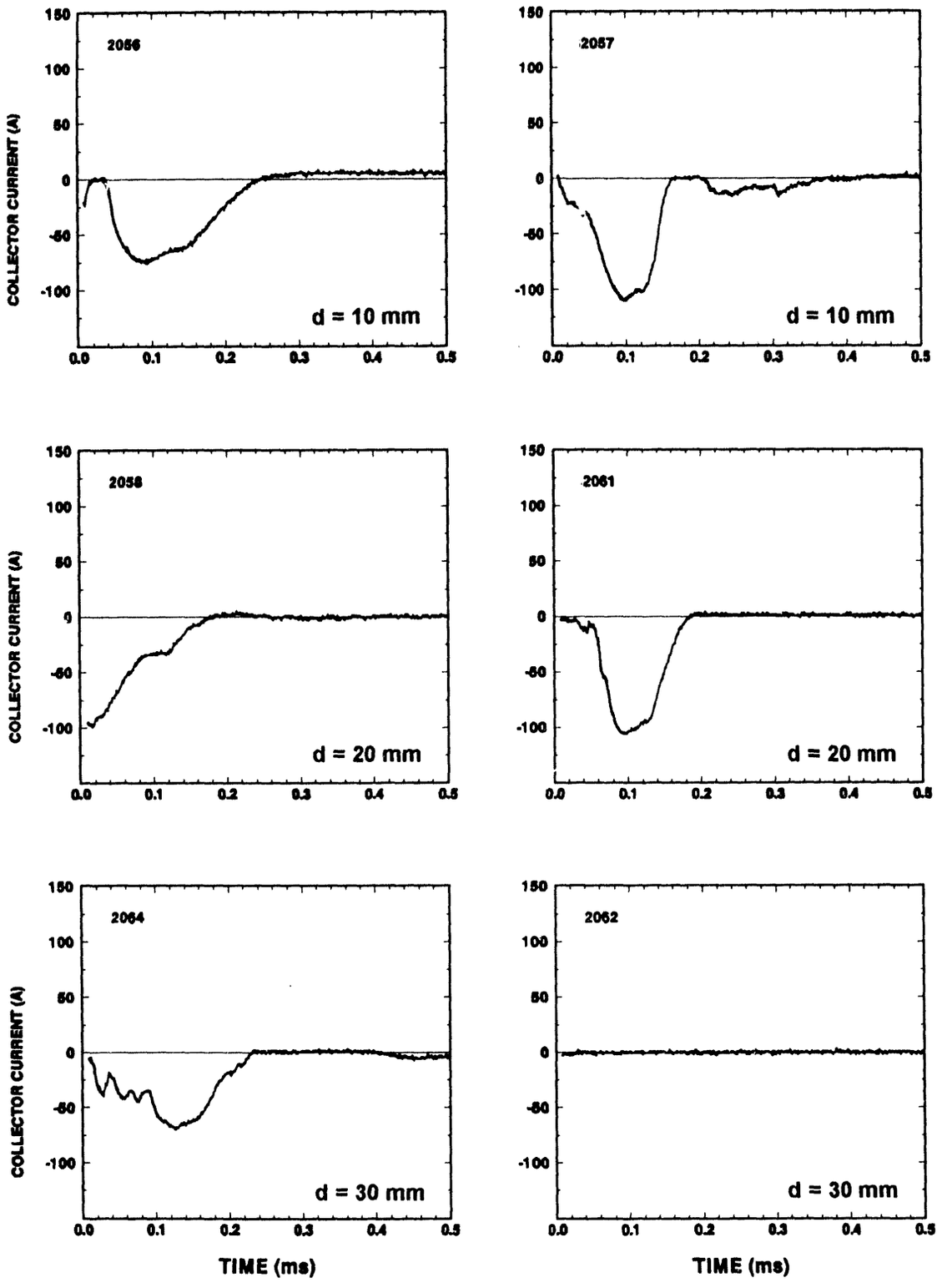

Figure 6-1 Interior collector currents recorded immediately after second return strokes following full burnthrough of the barrier plate. Shown are two examples obtained with varying barrier-to-collector distances d

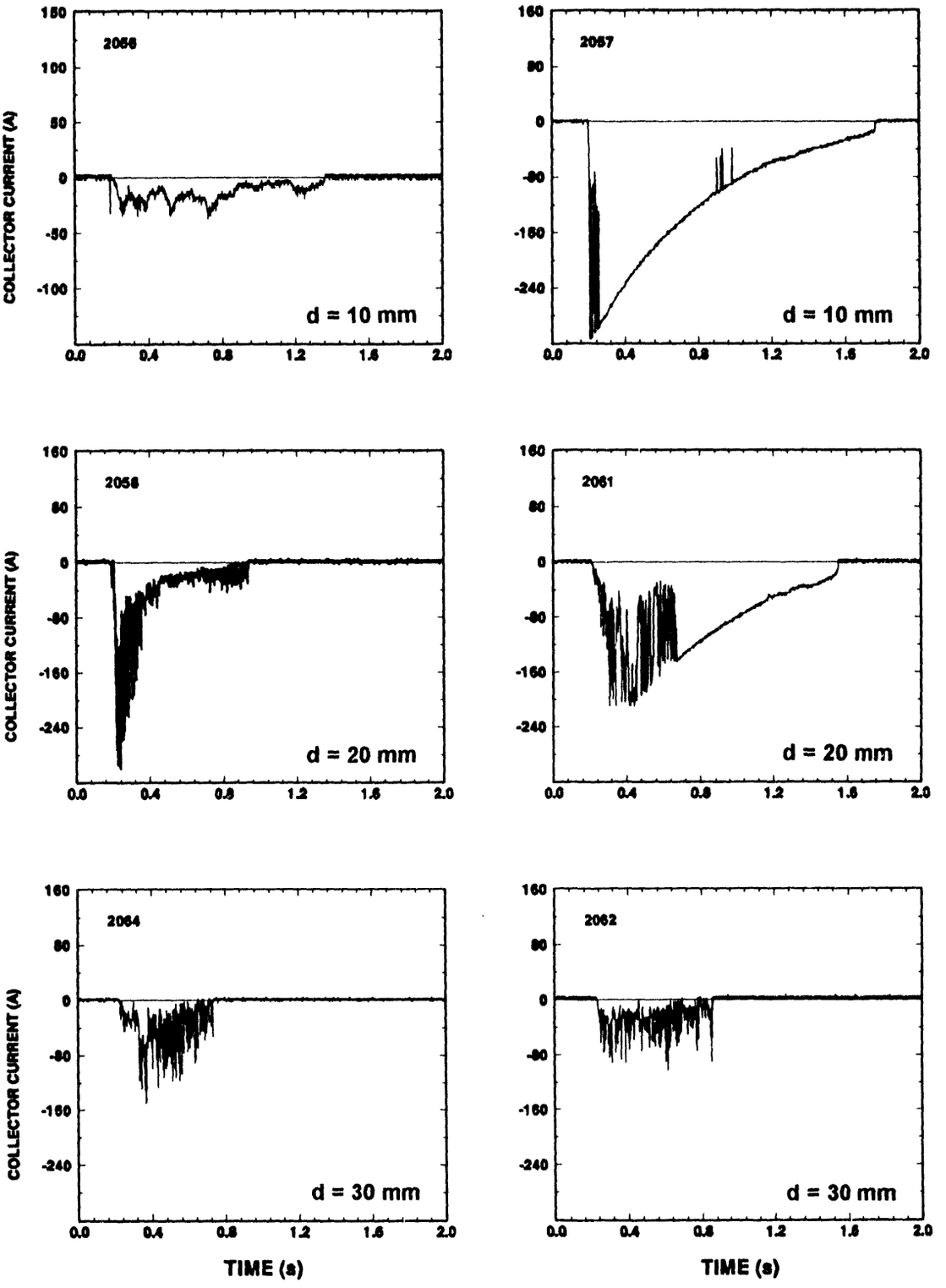

Figure 6-2 Interior collector currents of Figure 6-1 recorded on a longer time scale. First return strokes occur at approximately 100 ms into each record, and it is evident that no significant current reached the collector until the onset of the second stroke

7.0 Coupling to a Flat Detonator Cable Behind the Penetration Site

In order to investigate how much current couples onto a flat, flexline detonator cable located directly behind a lightning penetration site in the outer case of a weapon, the experimental fixture of Figure 3-4 was modified slightly as shown in Figure 7-1. The changes included the addition of a 0.063-in thick layer of silicone rubber over the exposed face of the brass collector cylinder to prevent any direct coupling to it from the penetrating arc. This coupling suppression approach was shown to be effective in separate tests with flash simulations comprised of both one and two return strokes and continuing currents. (Refer to the last two entries in Table 6-1.) A cross section of the test cable is shown in Figure 7-2. A short piece of braided conductor was soldered to each of the conductors of the cable, and, for the short-circuit current measurements, these were clamped to the supporting stem of the inner cylinder as indicated in Figure 7-1.

One measurement of short-circuit current was conducted using the instrumentation arrangement shown in Figure 3-6. Thus, configuration is different from that shown in Figure 3-4; specifically, the high impedance buffer amplifier was not required. In the present test, the barrier-to-cable distance was 0.2 in, and the applied current consisted of a 50-kA return stroke followed by continuing current of about 500-A initial amplitude. A response current of 69 A was recorded, a value nearly the same as was obtained during the similar tests in which current to the brass collector cylinder was measured. (See 3826, 3827, and 3832 in Table 6-1.) In actual weapons, the detonator circuit is typically tied to case ground at the firing set end, but floats at the detonator end. Under those conditions, any current injected onto the cable by means of the penetrating lightning arc would flow to case ground towards the firing set end of the cable and away from the detonator end. In situations where the firing circuit is entirely isolated from case ground, the maximum cable voltages that were obtained during the tests described below are so much lower than the kapton breakdown voltage that the probability of formation of a shorting arc to ground anywhere on the cable is diminishingly small.

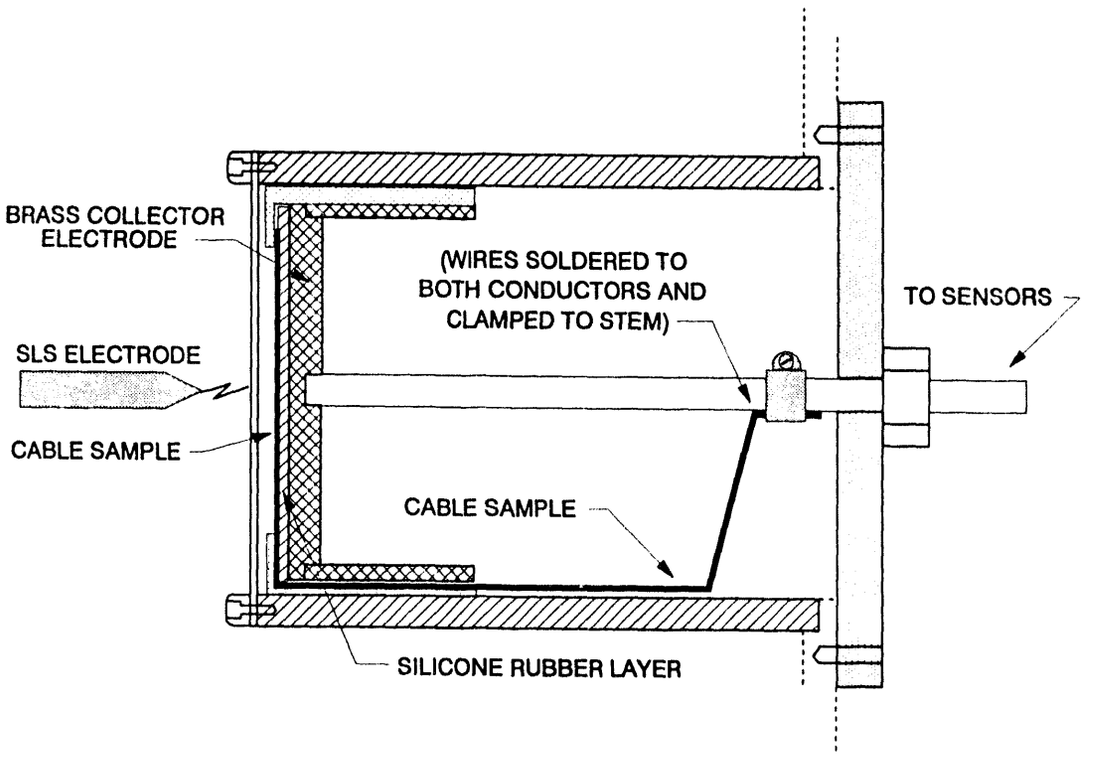

Figure 7-1 Experiment fixture configured for tests on the flat detonator cable

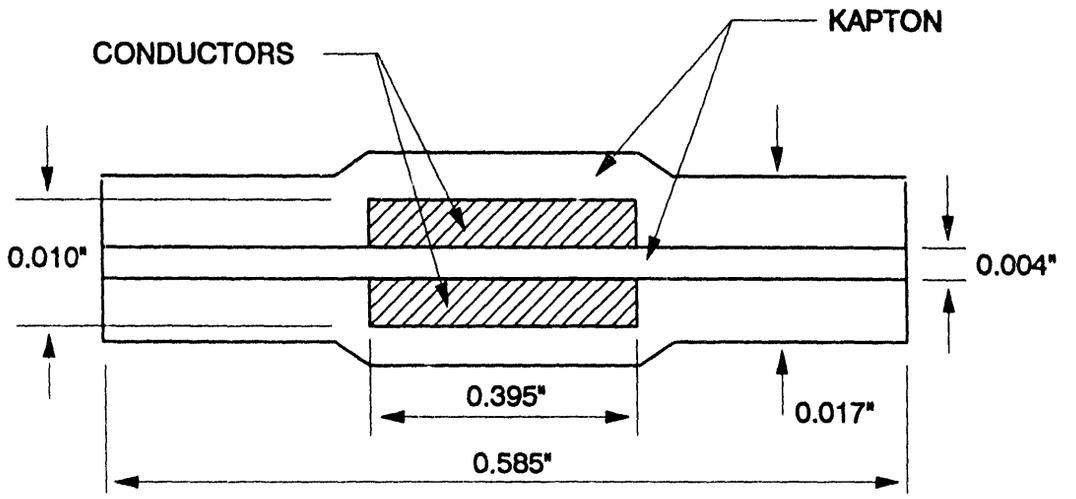

Figure 7-2 Cross section of flat detonator test cable

Voltages developed on the test sample were recorded using the instrumentation arrangement shown in Figure 7-3. Several test shots were made with the non-grounded end of the cable fed directly into the 50-Ω input resistance of the FOL transmitter. One shot was made with a 510-Ω resistor added in series as shown in Figure 7-3, which produced a result within about 16 percent of the average value obtained with the 50-Ω load. From this it was concluded that the source impedance of the voltage produced by the cable was considerably smaller than 50 Ω, and that the measurement into a 50-Ω load did not significantly perturb the open-circuit voltage developed on the cable. The data are summarized in Table 7-1. From these results it is apparent that the highest observed common-mode voltage was approximately 40 to 45 V, a level well below what would be required to initiate an exploding bridgewire detonator, even if applied as a differential source directly across the two conductors of the cable. Forty volts is also several orders of magnitude below the dielectric breakdown value of the kapton insulating layers of the cable, which is of the order of 5 - 7 kV.

Table 7-1.
Voltages Recorded on Detonator Cables
Following Barrier Penetration by Simulated Lightning

Test Shot ID	d[1] (in)	RS (kA)	I_{cc}[2] (A)	Meas. Voltage (V)	Comments
3433	0.2	53	464	Noise	Differential mode
3434	0.2	54	463	37	Common mode into 50 Ω
3435	0.2	454	455	41	
3840	0.2	56	494	39	
3841	0.2	42	497	41	
3842	0.2	52	509	46	Common mode into 560 Ω

[1] SLS electrode-to-barrier distance

[2] Initial amplitude of continuing current

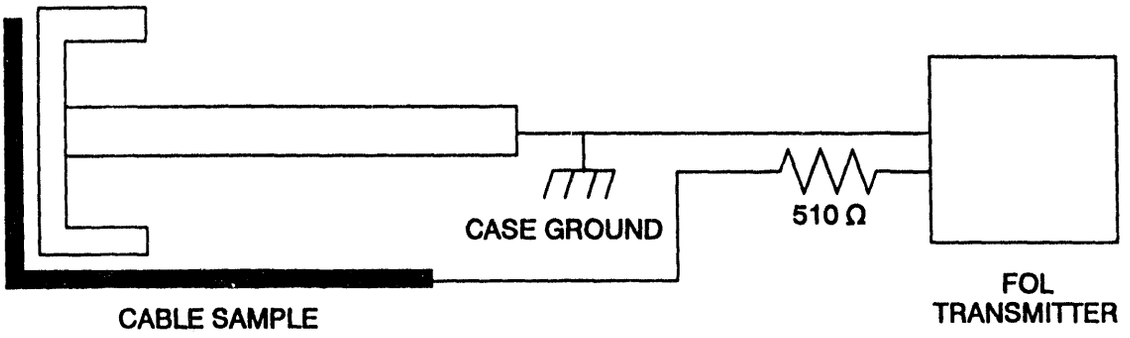

Figure 7-3 Instrumentation used in measuring voltages coupled to a flat detonator cable behind the site of a lightning penetration

8.0 Conclusion

Open-circuit voltages measured on either simulated structures or samples of flat detonator cables located behind the point of penetration of a metallic barrier penetrated by lightning are well below any level that is foreseen to create a threat to nuclear safety. On the other hand, it has been shown that a significant fraction of the incident continuing current flowing after barrier penetration has occurred can be injected onto either an internal structure or cable that is electrically grounded to the case. No occurrence of the injection of currents from return strokes occurring after barrier penetration was observed. Under circumstances in which small volumes of trapped gases exist behind penetration sites, rapid heating of the gas by subsequent return strokes has been shown to produce large mechanical impulses to the adjacent surfaces.

9.0 References

1. Fisher, R.J., "Stockpile Lightning Analysis and Test Plan (SLAT) Program: Technical Plan for Generic Experiments, Issue A," November 15, 1990.

2. Fisher, R.J. and G.H. Schnetzer, "Penetration of Metal Sheets by Simulated Lightning Currents," Sandia Report in process.

3. Fisher, R.J. and M.A. Uman, *Recommended Baseline Direct-Strike Lightning Environment for Stockpile-to-Target Sequences*, SAND89-0192, May 1989.

4. Phillpott, J. "Factors Affecting Puncture of Aluminum Alloy by Simulated Lightning," *Proc. Int. Conf. on Lightning and Static Electricity*, December 12-15, 1972.

5. Kern, A. "Simulation and Measurement of Melting Effects on Metal Sheets Caused by Direct Lightning Strikes," *Proc. Int. Aerospace and Ground Conf. on Lightning and Static Electricity*, Cocoa Beach, April 16-19, 1991.

6. Fisher, R.J. and G.H. Schnetzer, "Damage to Metallic Samples Produced by Measured Lightning Currents," *Proc. Int. Aerospace and Ground Conference on Lightning and Static Electricity*, Cocoa Beach, April 16-19, 1991.

7. Fisher, R.J., J.G. Kostas, and C. Chocas, *W82 Miscellaneous Lightning Burnthrough Tests*, Sandia Electromagnetic Test Report, December 9, 1988.

Distribution

1 AFGL
PL/GP/LYA
Attn: Dr. John Willet
Hanscom AFB, MA 01720

1 Philips Laboratory
GPAA
Attn: Dr. Stan Heckman
29 Randolph Rd.
Hanscom AFB, MA 01731-3010

5 Commander
USA Armament Research, Development,
and Engineering Center
Attn: SMCAR-FSN
SMCAR-AEC-IM
SMCAR-FSN-T
Picatinny Arsenal, NJ 07806-5000

1 Commander, US Army Armament, Munitions and Chemical Command
Attn: AMSC-MAY-W
Picatinny Arsenal, NJ 07806-5000

1 Office of the Assistant to the Secretary
of Defense (Atomic Energy)
Room 3E1074, The Pentagon
Washington, DC 20301-3050

3 Director
Defense Nuclear Agency
Attn: R. C. Webb
LTC Wayne Andrews
J. V. Brackett
Washington, DC 20305

1 Commander, Naval Sea Systems Command
Department of the Navy
Attn: Nuclear Weapons/Munitions
Sec Div (SEA-643)
Washington, DC 20360

1 Commander, Naval Sea Systems Command
Theater Nuclear Warfare Program (PMS 423)
Attn: T. Rosling
Washington, DC 20362-5101

Distribution (Continued)

4 Director, Strategic Systems Projects
Department of the Navy
Attn: B. Hannah
R. M. Jones
M. Whittaker
Ruth Ann Lee
Washington, DC 20376

1 US Department of Energy
Office of Military Applications
Attn: DP-22
Washington, DC 20545

2 Navy EOD Technology
Attn: Richard Burdette
Indian Head, MD 20640

2 Commander
NATC
Attn: M. Whitaker (SY84)
Patuxent River NAS, MD 20670

1 Commander, US Army Nuclear and Chemical Agency
Attn: MONA-MS (G. Long)
7500 Backlick Road
Springfield, VA 22150

1 RDA
Attn: Art Barondes
6940 S. Kings Highway
Alexandria, VA 22310

1 Dr. William Maurits
DDESB-KT
Hoffman Bldg. 1/Rm 856-C
2461 Eisenhower Ave.
Alexandria, VA 22331-0600

1 Commander
Naval Surface Weapon Center
Attn: B. Franklin
Dahlgren, VA 22448

1 Commander
Attn: HQ AFCESA (Fowler)
Tyndall AFB, FL 32403-6001

Distribution (Continued)

1 Commander
Attn: ASO/YQI (C. Churillo)
Eglin AFB, FL 32542

1 Commander, US Army Missile Command
Attn: Technical Library
Redstone Arsenal, AL 35898-5690

3 DoD SOTS
SMCAR-FSN-M
Attn: K. Haynes
Ft. McClellan, AL 36205-5300

1 Commander, US Army Armament, Munitions and Chemical Command
Attn: AMSMC-ASN-N
Rock Island, IL 61299-6000

1 National Severe Storms Laboratory
Storm Electricity and Cloud Physics
Attn: Dr. W. D. Rust
1313 Halley Circle
Norman, OK 73069

2 Field Command Defense Nuclear Agency
Attn: CDR F. T. Walker
Kirtland AFB, NM 87115-5000

1 US Department of Energy
Albuquerque Operations Office
Attn: NESD/WSSB
P.O. Box 5400
Albuquerque, NM 87115

4 Weapons Laboratory
Attn: D. Ulibarri/NTSW
M. Harrison/NTCA
LTCOL D. Stone/PL-LMI
Kirtland AFB, NM 87117-6006

1 Commander
NWEF
Attn: Jeff Stickney
Kirtland AFB, NM 87117

Distribution (Continued)

1 Logicon RDA
Attn: Bill Kehrer
P. O. Box 9377
Albuquerque, NM 87119

1 Los Alamos National Laboratory
Attn: Technical Library
M. G. Wheeler, WX-1
P.O. Box 1663
Los Alamos, NM 87545

1 Commander, White Sands Missile Range
Bldg. 21225
Attn: Technical Library
White Sands Missile Range, NM 88002

1 Headquarters
Air Force Inspection and Safety Center
Attn: SEWV (Blount)
Norton AFB, CA 924097

1 Electric Power Research Institute
Project Manager/Distribution Program
Attn: Ralph Bernstein
P. O. Box 10412
Palo Alto, CA 94303

3 University of California
Lawrence Livermore National Laboratory
Attn: Technical Info. Dept.
R. T. Hasbrouck
Bill Hubbel, L-125
R. A. Woelffer, L-125
P.O. Box 808
Livermore, CA 94550

Distribution (Continued)

1 MS 9001 C. T. Yokomizo (Org. 8007)
1 MS 9004 M. E. John (Org. 8100)
1 MS 9005 J. B. Wright (Org. 5300)
1 MS 9006 E. E. Ives (Org. 5200)
1 MS 9006 D. J. Bohrer (Org. 5303)
1 MS 9013 R. G. Miller (Org. 5366)
1 MS 9013 K. A. Mitchell (Org. 5366)
1 MS 9014 J. R. Hogan (Org. 5371)
1 MS 9014 D. L. Gehmlich (Org. 5371)
1 MS 9014 J. L. Mitchell (Org. 5371)
1 MS 9031 J. E. Marion (Org. 5302)
1 MS 9033 R. A. Pearson (Org. 5362)
1 MS 9033 G. E. Dietel (Org. 5362)
1 MS 9034 D. J. Beyer (Org. 5363)
1 MS 9035 G. C. Story (Org. 5365)
1 MS 9021 R. E. Martinell (Org. 8535)
1 MS 9202 L. E. Dighton (Org. 8116)
1 MS 9202 C. M. Furnberg (Org. 8116)
1 MS 9203 E. B. Talbot (Org 5354)
1 MS 9203 S. J. Vasey (Org. 5354)
1 MS 9222 C. A. Skinrood (Org. 8601)

1 MS 0311 R. F. Ellison, Jr. (Org. 2671)
1 MS 0319 S. B. Martin (Org. 2641)
1 MS 0319 J. H. Barnette (Org. 2905)
1 MS 0328 N. F. Siska (Org. 2674)
1 MS 0433 R. N. Brodie (Org. 25)
1 MS 0436 G. L. Maxam (Org. 5147)
1 MS 0447 J. S. Clabaugh (Org. 5111)
1 MS 0447 H. T. Lehman (Org. 5111)
1 MS 0455 G. R. Otey (Org. 4100)
1 MS 0459 T. S. Edrington (Org. 5205)
1 MS 0459 C. C. Burks (Org. 5203)
1 MS 0465 J. F. Ney (Org. 5003)
1 MS 0467 K. D. Nokes (Org. 5091)
1 MS 0469 D. F. McVey (Org. 5209)
1 MS 0471 J. P. Abbin, Jr. (Org. 5093)
1 MS 0482 K. Oishi (Org. 5161)
1 MS 0490 S. D. Spray (Org. 12331)
1 MS 0492 R. E. Church (Org. 12332)
1 MS 0492 G. A. Sanders (Org. 12332)
1 MS 0492 P. E. D'Antonio (Org. 12324)
1 MS 0492 J. F. Wolcott (Org. 12332)
1 MS 0492 D. Loescher (Org. 12332)
1 MS 0507 K. G. McCaughey (Org. 2700)
1 MS 0511 G. N. Beeler Org. 2500)
1 MS 0513 H. W. Schmitt (Org. 2000)

Distribution (Continued)

1	MS 0523	R. D. Holt (Org. 2251)
1	MS 0523	R. E. Kreutzfeld (Org. 5111)
1	MS 0523	J. O. Harrison (Org. 2251)
1	MS 0527	L. A. Andrews (Org. 2235)
1	MS 0570	C. W. Childers (Org. 5900)
1	MS 0755	H. W. Church (Org. 6612)
1	MS 0761	P. E. Rexroth (Org. 5822)
1	MS 0765	D. E. McGovern (Org. 5821)
1	MS 0768	J. W. Kane (Org. 5806)
1	MS 0865	M. E. Morris (Org. 2753)
1	MS 0865	K. C. Chen (Org. 2753)
75	MS 0865	R. J. Fisher (Org. 2753)
2	MS 0865	R. D. Jones (Org. 2753)
1	MS 0865	R. E. Jorgenson (Org. 2753)
1	MS 0865	K. O. Merewether (Org. 2753)
10	MS 0865	G. H. Schnetzer (Org. 2753)
1	MS 0865	L. K. Warne (Org. 2753)
1	MS 0971	G. H. Mauth (Org. 9203)
1	MS 1007	J. F. Jones, Jr. (Org. 2172)
1	MS 1073	P. V. Dressendorfer (Org. 2277)
1	MS 1153	L. D. Bacon (Org. 1248)
1	MS 1165	J. E. Powell (Org. 9300)
1	MS 1166	J. H. Renken (Org. 9352)
1	MS 1166	G. J. Scrivner (Org. 9306)
1	MS 1166	C. D. Turner (Org. 9352)
1	MS 1166	C. N. Vittitoe (Org. 9352)
1	MS 1181	J. M. Hoffman (Org. 1208)
1	MS 1188	R. G. Adams (Org. 1275)

1	MS 9018	Central Technical Files (Org. 8523-2)
5	MS 0899	Technical Library (Org. 7141)
1	MS 0619	Technical Publications (Org. 7151)
10	MS 0100	Document Processing (for DOE/OSTI) (Org. 7613-2)

DATE
FILMED
11/2/94

END